Optical Engineering

OpticalEngineering.SPIEDigitalLibrary.org

Thermal compensation design of truss structure for large-scale off-axis three-mirror space telescope

Lin Yang
Lei Wei
Lei Zhang

SPIE.

Lin Yang, Lei Wei, Lei Zhang, "Thermal compensation design of truss structure for large-scale off-axis three-mirror space telescope," *Opt. Eng.* **58**(2), 023109 (2019), doi: 10.1117/1.OE.58.2.023109.

Optical Engineering 58(2), 023109 (February 2019)

Thermal compensation design of truss structure for large-scale off-axis three-mirror space telescope

Lin Yang,[a,b,c] Lei Wei,[c] and Lei Zhang[a,b,c,*]
[a]Chinese Academy of Sciences, Changchun Institute of Optics, Fine Mechanics and Physics, Changchun, China
[b]University of Chinese Academy of Sciences, Beijing, China
[c]Chang Guang Satellite Technology Ltd. Co., Changchun, China

Abstract. The image quality of the large-scale, long-focus, large field of view, off-axis three-mirror anastigmat space telescope will decrease dramatically due to the thermal effect. This paper studies the thermal deformation of the telescope, and based on its axial deformation, it proposes a passive thermal compensation design using truss rods made of carbon fiber-reinforced plastics, utilizing its thermal conducting design, which is determined by different spread quantity and spread angle of the lamination. Meanwhile, it satisfies the system stiffness requirement. First, the truss rods are divided into several independent triangles, according to the principle of equal axial distance after deformation, the function in terms of coefficient of thermal expansion (CTE) and length of truss rods is determined. Bonded by the optical tolerance requirement, the range of the CTE is obtained. Second, according to the CTE function, coupled with the stiffness requirement of the whole instrument, the CTE of each truss rod is determined. According to the CTE and stiffness requirement, the design of truss rods lamination is carried out. Finally, the group of truss rods with unequal CTE is obtained. The results have been validated by finite element analysis, vibration experiments, and image test, which indicate that the accuracy of the space telescope studied meets the requirements of optical tolerance; in addition, the rotation angle of the front panel around the X axis is competent, implying the stiffness requirement is solved. Moreover, the modulation transfer function at Nyquist frequency is better than 0.178 under the condition of 20°C ± 5°C. [DOI: 10.1117/1.OE.58.2.023109]

Keywords: long focus; three-mirror anastigmat; space telescope; lamination design; thermal compensation design; modulation transfer function.

Paper 181226 received Aug. 28, 2018; accepted for publication Jan. 25, 2019; published online Feb. 20, 2019.

1 Introduction

With the development of Earth observation technology, the three-mirror anastigmat (TMA) optical system has been widely studied by researchers all over the world because of its advantages of no center obscuration, high-energy utilization, easy-to-achieve wide field of view, and high resolution. However, due to the asymmetry of its optical system, its supporting structural design, installation, and adjustment technologies are generally recognized as a technical difficulty in comparison with the symmetrical structure of the coaxial optical systems.[1]

The truss structure is widely used in the main support system of large and medium space telescope for its advantages of light weight, high stiffness ratio, and easy-to-manufacture characteristics. For example, the large space remote sensors, such as the Hubble, SPOT, HI-RISE, and ALOS-3, in the United States have adopted the truss structure.[2–4] It is difficult for the space telescope to maintain a relatively constant temperature environment due to the uneven acceptance of radiation heat on the surface during its on-orbit operation. The changeable thermal environment leads to the deformation of the space telescope under the influence of thermal strain effect, which consequently incur defocusing and deviation of the optical system.[5,6] Therefore, for the high-resolution telescope, it is necessary for its structure support system to adopt thermal compensation design.

In this paper, truss structure is used as the main supporting structure of this large-scale TMA optical system space telescope. To meet the imaging requirement of 20°C ± 5°C, the coefficient of thermal expansion (CTE) of truss rods is analyzed and determined by means of passive thermal compensation technique. Based on this, the carbon fiber-reinforced plastics (CFRP) lamination technology is used for analyzing and determining the CTE of the truss rods. The CFRP lamination of truss rods is designed to meet the requirements of thermal deformation and stiffness. Validated by finite element analysis, experiments, and tests, the space telescope studied in this paper has good thermal stability, stiffness, and imaging ability, which is a key comprehensive and indirect indicator which shows that the compensation design is effective.[7,8]

2 Determination of CTE of Truss Rods

To eliminate the influence of thermal effect on the optical system of space telescope, it is necessary to take measures to compensate the optical system so that it can keep a satisfactory imaging quality within a large temperature range. This method is normally referred to as heat-free design or thermal compensation technology. At present, passive thermal compensation technology is the most adopted method for space telescope.[9,10] Its characteristics are described as simple structure, small size, light mass, zero power consumption, and high reliability. Its principle is to eliminate the influence of thermal effect by the orderly combination of different materials and take the advantage of the difference

*Address all correspondence to Lei Zhang, E-mail: cullencaptain@163.com

0091-3286/2019/$25.00 © 2019 SPIE

among various material properties so as to obtain the heat-free effect.[11] This paper aims to present a passive thermal compensation technology by utilizing CFRP material to minimize the thermal deformation effect on the whole instrument.

2.1 *Maximum Axial Deformation Constraints*

The optical system of the TMA space telescope studied in this paper is shown in Fig. 1. Built on the optical system layout, the truss structure is designed as shown in Fig. 2. The weight of this space telescope is >750 kg and the dimension is $1660 * 1580 * 1700$ mm as marked. The truss rods are labeled from truss 1 to truss 8. Other rods not labeled share the same name due to symmetry.

The thermal deformation principle diagram of space telescope studied in this paper is shown in Fig. 3 below. In this paper, the thermal deformation of each mirror and the front and back panels made of titanium alloy is regarded as a black box and considered as a constant under the condition that the change in temperature is 5°C and the CTE of titanium is $9 \times 10^{-6}/°C$. The space telescope can work well only if the position accuracy of each mirror meets the optical tolerance shown in Table 1. The thermal deformation of the space telescope on orbit shall be extended in three directions of X, Y, and Z, respectively, in which the optical axis parallel to Z is perpendicular to the X–Y plane. It can be seen from Figs. 2 and 3 that the mirrors are mounted to the front and back panels, and that the materials of each mirror component have been determined. This paper mainly studies the thermal compensation in the direction of optical axis (Z direction), and because the primary and the tertiary mirrors are installed on the same back panel, the secondary mirror and the plane mirror are mounted on the same front panel, thermal compensation structure of truss rods is specially designed to work for the distance from the secondary and plane mirrors to the primary and tertiary mirrors.

In this paper, the thermal deformation of the mirror base components and the front and back panels is regarded as a known constant, which is caused by the thermal deformation of the panels and the mirror base components made of titanium alloy. All truss rods are connected to the panels made of titanium alloy using epoxy resin with an elasticity modulus of 4.5 Mpa, whereas the elasticity modulus of CFRP and titanium alloy are all better than 80 Gpa. The ratio between them can be almost 20,000:1. Under this circumstance, the thermal deformation of panels can be considered exempt from the constraint of the truss rods. Therefore, the

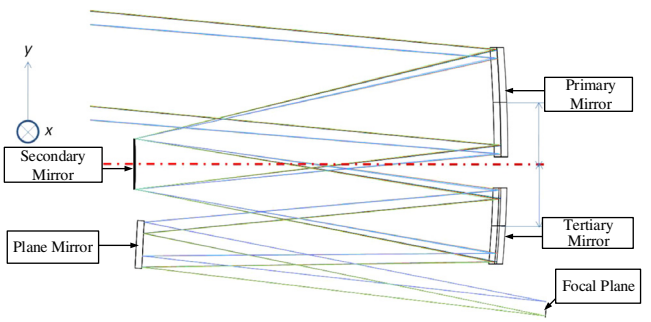

Fig. 1 Optical system layout.

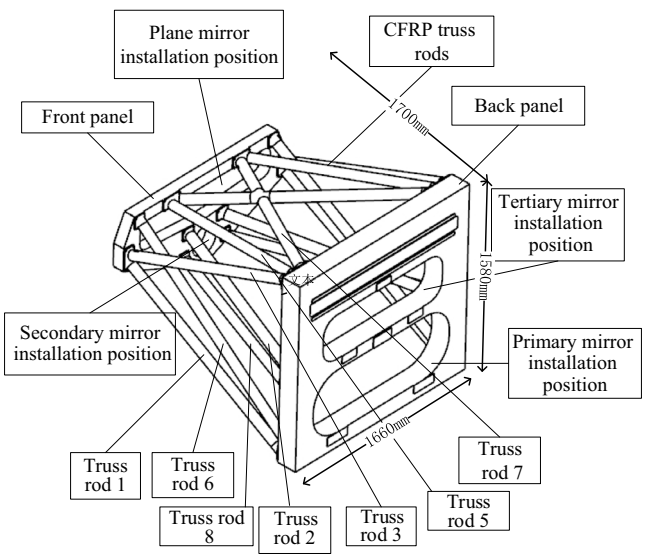

Fig. 2 Optimized model of main support structure of the space telescope.

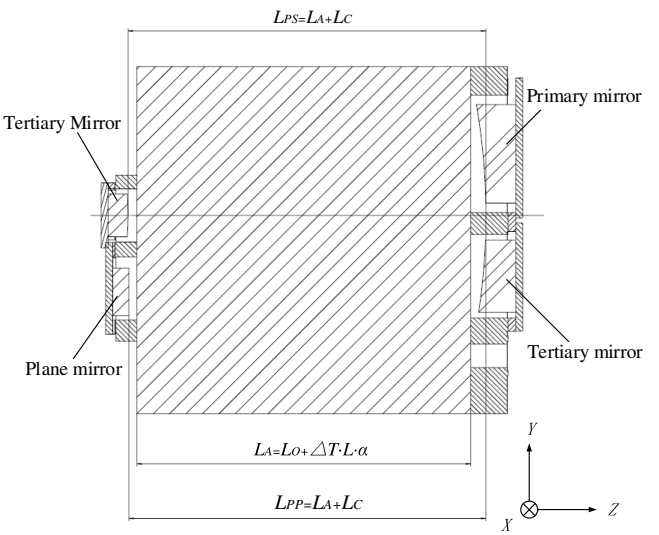

Fig. 3 Thermal deformation principle diagram.

Table 1 Requirement of optical tolerance compared to primary mirror.

Variance	Primary mirror	Secondary mirror	Tertiary mirror	Plane mirror
ΔX (mm)	Datum	0.03	0.03	—
ΔY (mm)	Datum	0.03	0.03	—
ΔZ (mm)	Datum	0.04	0.04	—
θX (″)	Datum	13	15	30
θY (″)	Datum	13	15	30
θZ (″)	Datum	20	20	—

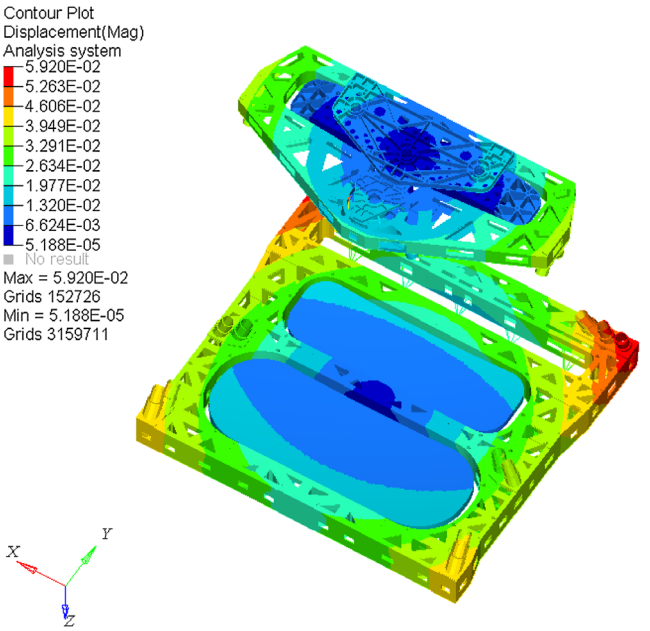

Fig. 4 Cloud chart of thermal deformation without truss rods.

Table 2 The analysis results of the optical eccentricity and the tilt of mirror components.

Variance	Primary mirror	Secondary mirror	Tertiary mirror	Plane mirror
ΔX′ (mm)	Datum	0.00	0.00	0.00
ΔY′ (mm)	Datum	0.0129	0.0258	0.0022
ΔZ′ (mm)	Datum	0.0010	0.006	0.0013
θX′ (″)	Datum	2.348	2.42	3.69
θY′ (″)	Datum	0.00	0.00	0.00
θZ′ (″)	Datum	0.00	0.00	0.00

deformation analysis can be carried out without the truss rods and when all panels and mirror component are in the right installation place. The results of the analysis, the optical eccentricity, and the tilt of these mirror components are shown in Fig. 4 and Table 2. Because of the asymmetry of off-axis system, coupled with weight caused by the plane and secondary mirror components mounted on the front panel which looks like a cantilever, a rotation of the front panel is inclined to happen. To avoid this, the length of all the truss rods must be equal in the direction of Z after thermal deformation.

To sum up, after the thermal deformation of the truss rods, the following conditions should be met:

(1) $|\Delta T \cdot L_O \cdot \alpha| \leq \gamma.$ (1)

(2) All trusses must have the same Z axial distance after thermal deformation.

(3) Modulation transfer function (MTF) at Nyquist frequency with the temperature range of 20°C ± 5°C should be better than 0.175.

Here, ΔT is the temperature variation, which is 5°C in this paper; L_o is the axial length of truss rods as a whole; and α is the comprehensive CTE of all, by comprehensive it means that the CTE has considered the thermal effect of the panels made of titanium. Here, γ is the maximum deformation of all truss rods, which should be

$$\gamma = \Delta Z - \Delta Z'_{PS}, \tag{2}$$

where ΔZ is the tolerance of Z axial between the primary and the secondary mirrors, and $\Delta Z'_{\mathrm{PS}}$ is the tolerance of Z axial between the primary and the secondary mirrors caused by thermal influence only by mirror base components and panels made of titanium, but without the influence of the truss rods. Since the temperature variation is 5°C and the CTE of titanium is 9×10^{-6}/°C, then $\Delta Z'_{\mathrm{PS}}$ is obtained as 1 μm. The results are shown in Table 2. Therefore, the theoretical γ is about 0.04 mm, where we set a safety coefficient as 1.33 which in turn determines γ as 0.03 mm.

According to the optical system shown in Fig. 1, we establish the finite element model (FEM) of the main support structure of researched space telescope, which is shown in Fig. 3. The definition is shown below:

L_O means the original length of the truss rods in Z direction without thermal influence.

L_A means the length with thermal influence.

L_C means the sum of deformation of front panel, back panel, mirror base, and truss rod junction made of titanium caused by thermal influence.

L_{PS} means the distance between primary and secondary mirrors under the condition of thermal influence.

L_{PP} means the distance between primary and plane mirrors under the condition of thermal influence.

2.2 *CTE Determination*

After the determination of maximum axial deformation, the CTE is to be concluded. The truss structure studied in this paper is divided into the triangles as shown in Figs. 5–10.

Since all the M which represents the length of Z axis are the same after deformation, the problem function is listed in function 3. It should be noted that the α_i different from each other because of the asymmetric structure:

$$\begin{cases} l_1^2(1+\Delta T\cdot\alpha_1)^2 - A^2 = l_3^2(1+\Delta T\cdot\alpha_3)^2 - B^2 \\ l_5^2(1+\Delta T\cdot\alpha_5)^2 - E^2 - F^2 = l_3^2(1+\Delta T\cdot\alpha_3)^2 - B^2 \\ l_7^2(1+\Delta T\cdot\alpha_7)^2 - D^2 = l_5^2(1+\Delta T\cdot\alpha_5)^2 - E^2 \\ l_6^2(1+\Delta T\cdot\alpha_6)^2 - G^2 = l_3^2(1+\Delta T\cdot\alpha_3)^2 - B^2 \\ l_8^2(1+\Delta T\cdot\alpha_8)^2 - H^2 = l_3^2(1+\Delta T\cdot\alpha_3)^2 - B^2 \\ l_2^2(1+\Delta T\cdot\alpha_2)^2 - J^2 - N^2 = l_3^2(1+\Delta T\cdot\alpha_3)^2 - B^2 \end{cases}. \tag{3}$$

The length of M is the vertical distance in the direction of Z and it is also the projection distance of M'. The solution of the above equation shows that the magnitude order of CTE α is 10^{-6}, so the α^2 terms in the equation can be ignored, and the following function is obtained:

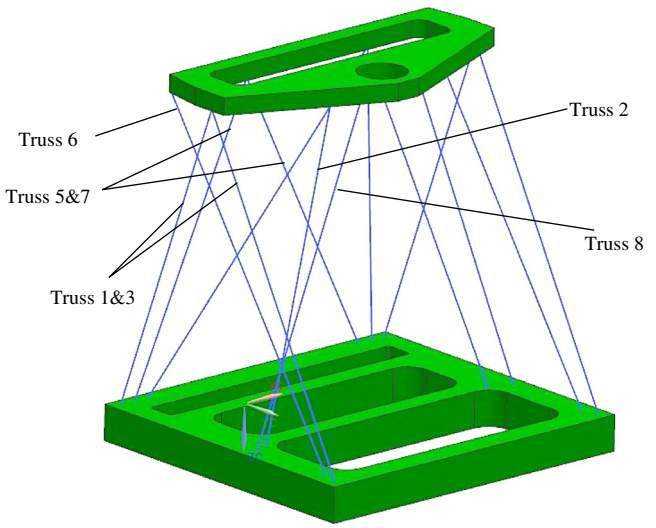

Fig. 5 Simplified truss structure.

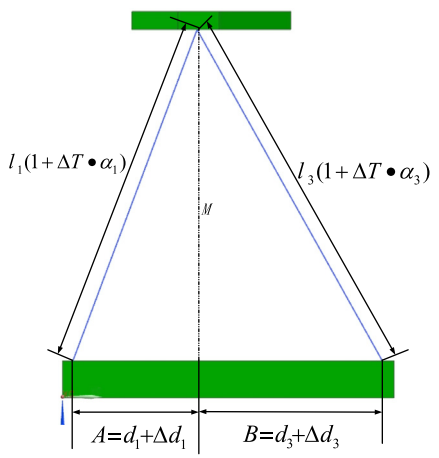

Fig. 6 Triangle of truss rods 1 and 3.

$$\begin{cases} \alpha_1 = \frac{1}{2\Delta T}\left[\left(\frac{l_3}{l_1}\right)^2(1+2\Delta T\cdot\alpha_3)+\frac{A^2-B^2}{l_1^2}-1\right] \\ \alpha_7 = \frac{1}{2\Delta T}\left[\left(\frac{l_5}{l_7}\right)^2(1+2\Delta T\cdot\alpha_5)+\frac{D^2-E^2}{l_5^2}-1\right] \\ \alpha_5 = \frac{1}{2\Delta T}\left[\left(\frac{l_3}{l_5}\right)^2(1+2\Delta T\cdot\alpha_3)+\frac{E^2+F^2-B^2}{l_5^2}-1\right] \\ \alpha_6 = \frac{1}{2\Delta T}\left[\left(\frac{l_3}{l_6}\right)^2(1+2\Delta T\cdot\alpha_3)+\frac{G^2-B^2}{l_6^2}-1\right] \\ \alpha_8 = \frac{1}{2\Delta T}\left[\left(\frac{l_3}{l_8}\right)^2(1+2\Delta T\cdot\alpha_3)+\frac{H^2-B^2}{l_8^2}-1\right] \\ \alpha_2 = \frac{1}{2\Delta T}\left[\left(\frac{l_3}{l_2}\right)^2(1+2\Delta T\cdot\alpha_3)+\frac{N^2+J^2-B^2}{l_2^2}-1\right] \end{cases}. \quad (4)$$

In Eqs. (3) and (4), l_1 to l_7 represents the length of the truss rod without thermal expansion. α_1 to α_7 are the CTE of the respective truss rod in the axial direction. A, B, D, E, F, G, H, J, and N, shown in Figs. 5–9, are the projection distance of each truss rod in the X–Y plane after thermal deformation. The length of A, B, D, E, F, G, H, J, and N can be expressed in the following Eq. (5):

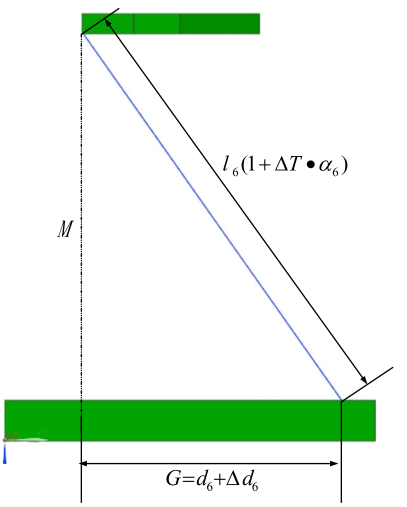

Fig. 7 Triangle of truss rod 6.

$$\begin{aligned} A &= d_1+\Delta d_1 & G &= d_6+\Delta d_6 \\ B &= d_3+\Delta d_3 & H &= d_8+\Delta d_8 \\ D &= d_7+\Delta d_7 & J &= d_2+\Delta d_2 \\ E &= d_5+\Delta d_5 & N &= d_2'+\Delta d_2' \\ F &= d_{57}+\Delta d_{57} \end{aligned} \quad (5)$$

Among them, d_1 to d_7 are the projection distance of the truss rod in the X–Y plane when the truss structure is not subjected to thermal deformation, Δd_1 to Δd_7 are the variations of the projection distance of the truss rods in the X–Y plane after the truss structure is subjected to thermal deformation. The distance between the installation points of the truss rods is known because of the change of the distance between the installation points of the truss rods on the front and back panels. The combination of Eqs. (5) and (4) leads to Eq. (6):

$$\begin{cases} \alpha_1 = \left(\frac{l_3}{l_1}\right)^2\alpha_3+\frac{\Delta d_1^2-\Delta d_3^2+2(d_1\Delta d_1-d_3\Delta d_3)}{2\Delta T l_1^2} \\ \alpha_7 = \left(\frac{l_5}{l_7}\right)^2\alpha_5+\frac{\Delta d_7^2-\Delta d_5^2+2(d_7\Delta d_7-d_5\Delta d_5)}{2\Delta T l_7^2} \\ \alpha_5 = \left(\frac{l_3}{l_5}\right)^2\alpha_3+\frac{\Delta d_5^2+\Delta d_{57}^2-\Delta d_3^2+2(d_5\Delta d_5+d_{57}\Delta d_{57}-d_3\Delta d_3)}{2\Delta T l_5^2} \\ \alpha_6 = \left(\frac{l_3}{l_6}\right)^2\alpha_3+\frac{\Delta d_6^2-\Delta d_3^2+2(d_6\Delta d_6-d_3\Delta d_3)}{2\Delta T l_6^2} \\ \alpha_8 = \left(\frac{l_3}{l_8}\right)^2\alpha_3+\frac{\Delta d_8^2-\Delta d_3^2+2(d_8\Delta d_8-d_3\Delta d_3)}{2\Delta T l_8^2} \\ \alpha_2 = \left(\frac{l_3}{l_2}\right)^2\alpha_3+\frac{\Delta d_2^2+\Delta d_2'^2-\Delta d_3^2+2(d_2\Delta d_2+d_2\Delta d_2'-d_3\Delta d_3)}{2\Delta T l_2^2} \end{cases}. \quad (6)$$

Since the variation of Δd is 10^{-2} mm level and the rod length l is 103 mm, the following polynomial composed of Δd^2 divided by the denominator is almost 10^{-10} in magnitude, which can be ignored. In the same way, as the magnitude order of d_1 to d_7 is almost 10^2, ΔT is 5°C, which means that the denominator is 10^7 in magnitude order, the number with 10^{-8} magnitude order can also be ignored. To sum up, Eq. (6) can be simplified to Eq. (7):

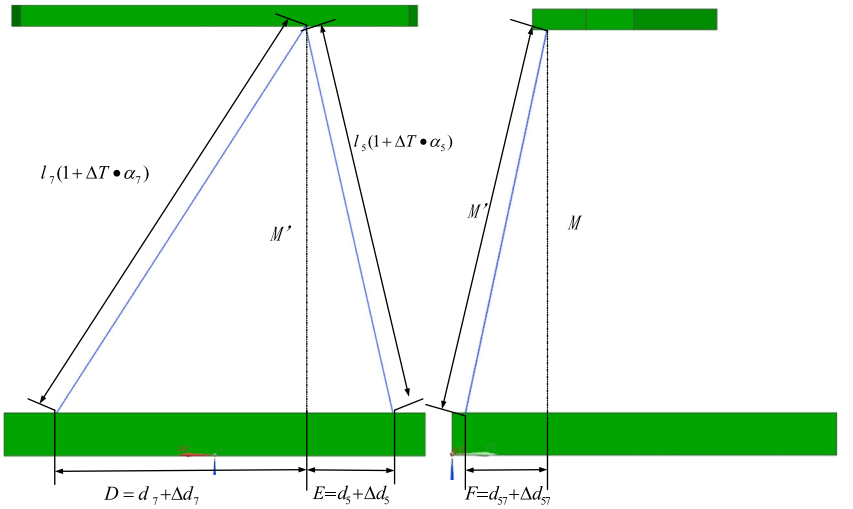

Fig. 8 Triangle of truss rods 5 and 7.

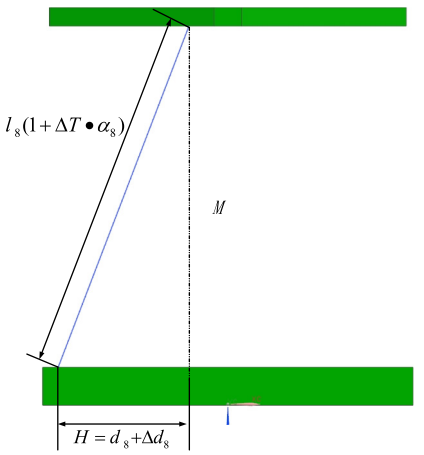

Fig. 9 Triangle of truss rod 8.

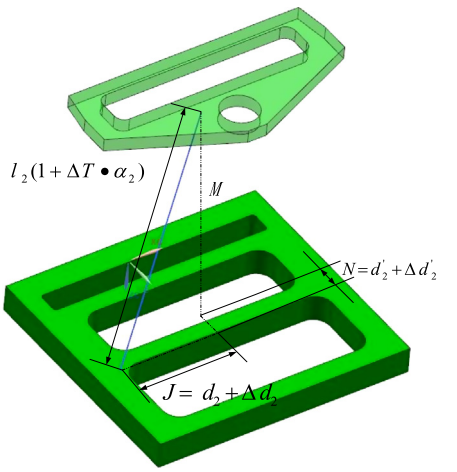

Fig. 10 Triangle of truss rod 2.

$$\begin{aligned}
\alpha_1 &= \left(\frac{l_3}{l_1}\right)^2\alpha_3 \qquad \alpha_6 = \left(\frac{l_3}{l_6}\right)^2\alpha_3 \\
\alpha_7 &= \left(\frac{l_5}{l_7}\right)^2\alpha_3 \qquad \alpha_8 = \left(\frac{l_3}{l_8}\right)^2\alpha_3 . \\
\alpha_5 &= \left(\frac{l_3}{l_5}\right)^2\alpha_3 \qquad \alpha_2 = \left(\frac{l_3}{l_2}\right)^2\alpha_3
\end{aligned} \tag{7}$$

It can be concluded from Eq. (7) that all the CTE of the truss rods can be converted into a function related to α_3, as long as α_3 is determined, all the other coefficient can be determined.

Since the thermal deformation of the truss rods must satisfy Eq. (1), the thermal deformation of the truss rod 3 must satisfy the following Eq. (8):

$$|M - M_O| \le \gamma. \tag{8}$$

where M_O is the axial distance of the truss rod without thermal deformation, which is already known. Here, M is the axial distance of the truss rod after thermal deformation. For truss rod 3, there is

$$M^2 = l_3^2(1 + \Delta T \cdot \alpha_3)^2 - B^2. \tag{9}$$

Combining Eqs. (8)–(10) acquires the following equation:

$$\begin{aligned}
\frac{1}{\Delta T}\left[\frac{\sqrt{(M_O-\gamma)^2+B^2}}{l_3}-1\right] \le \alpha_3 \\
\le \frac{1}{\Delta T}\left[\frac{\sqrt{(M_O+\gamma)^2+B^2}}{l_3}-1\right].
\end{aligned} \tag{10}$$

By introducing specific values in Eqs. (7) and (10), the range of the CTE of the truss rods is obtained:

$$\begin{cases}
\alpha_1 = 1.152\alpha_3 \\
\alpha_7 = 1.278\alpha_3 \\
\alpha_5 = 0.961\alpha_3 \\
\alpha_6 = 1.306\alpha_3 \\
\alpha_8 = 1.006\alpha_3 \\
\alpha_2 = 0.996\alpha_3 \\
-1.7\times10^{-6}/^{\circ}\mathrm{C} \le \alpha_3 \le 5.4\times10^{-6}/^{\circ}\mathrm{C}
\end{cases} . \tag{11}$$

To facilitate the lamination design, the CTE of Eq. (11) is rounded up and Eq. (12) is obtained as the final function of the thermal expansion coefficients of the rods:

$$\begin{cases} \alpha_1 = 1.2\alpha_3 \\ \alpha_7 = \alpha_6 = 1.3\alpha_3 \\ \alpha_5 = \alpha_3 = \alpha_8 = \alpha_2 \\ -1.7 \times 10^{-6}/\text{°C} \le \alpha_3 \le 5.4 \times 10^{-6}/\text{°C} \end{cases}. \tag{12}$$

3 Lamination Design for Truss Rods

The spread quantity and spread angle of the lamination design of truss rods is the core of the structural design, and the quality of the lamination will determine the success of truss design to a great extent. Lamination design is built on the orientation of each unidirectional layer in the laminate, layer sequence, percentage of each unidirectional layer in total number of layers, the total number of layers, etc. The widely applied theoretical functions for the single laminate are as follows:[12]

The vertical elastic modulus:

$$E_1 = E_t V + E_m(1 - V_t). \tag{13}$$

The lateral elastic modulus:

$$E_2 = \frac{E_f E_m (V_f + \eta_2 V_m)}{E_m V_f + E_f V_m \eta_2)}. \tag{14}$$

The vertical Poisson's ratio:

$$\nu_1 = \nu_f V_f + V_m(1 - V_f). \tag{15}$$

The lateral Poisson's ratio:

$$\nu_2 = \nu_1 \frac{E_1}{E_2}. \tag{16}$$

The vertical and lateral shear modulus:

$$G_{12} = \frac{G_f G_m (V_f + \eta_{12} V_m)}{G_m V_f + G_f V_m \eta_{12})}. \tag{17}$$

The E_f, E_m are the elastic modulus of carbon fiber and matrix, respectively; v_f, v_m are the Poisson's ratios; G_f, G_m are the shear modulus; V_f is the volume of the fiber; $V_m = 1 - V_f$ is the volume matrix; η_2 and η_{12} are the correction coefficients obtained from experiments, and the carbon fiber/cyanate may use 0.7.[12] Since the truss structure designed in this paper needs a higher base frequency to evade the inherent frequency of the rocket itself, the high modulus fiber M40 is preferred and the resin material adopted is cyanate. Accordingly, the unidirectional material parameters of the carbon fiber are shown in Table 3.

The most commonly used laminating design for simple parts like truss rods is meshed laminates. the most commonly used way. That means, layers shall be plied in $\pm\theta$o direction, and this method is adopted in this paper. The cross-layer often uses Halpin function to calculate the CTE in the central direction of the laying angle from $-\theta$o to $+\theta$o.[13]

In this project, the CFRP material of truss rod is equivalent to isotropic material and its equivalent modulus is 70 Gpa. The thickness of all truss rods are obtained by previous optimization under requirements like strength and stiffness. The concrete values are shown in Table 4.

According to the above analysis, the layer design of truss rods in this paper should meet the requirement of Eq. (12). Owing to the need to set α_3 first and to make the truss rods with a high axial modulus, this paper selects the ± 15 deg as the spread angle and the single layer thickness of 0.4 mm as the design for rod 3. Through analysis, the key parameters of the rod 3 are obtained and listed in Table 5.

It is clear that the axial linear expansion of rod 3 satisfies the requirement of Eq. (12). The axial coefficient of the rest of the rods can be calculated according to equation relationships between truss rods. the result is shown in Eq. (18):

$$\begin{cases} \alpha_1 = -2.016 \times 10^{-6}/\text{°C} \\ \alpha_7 = \alpha_6 - 2.184 \times 10^{-6}/\text{°C} \\ \alpha_5 = \alpha_3 = \alpha_8 = \alpha_2 = -1.68 \times 10^{-6}/\text{°C} \end{cases}. \tag{18}$$

According to Eq. (18), taking process technology into consideration, the spread angle is rounded up to carry out the layer lamination. Through the orderly design of the lamination angle, the thickness of the unidirectional layer and the number of layers, the layout of the truss rod is obtained as shown in Table 6.

Table 4 Thickness of truss rods.

T1 (mm)	T2 (mm)	T3 (mm)	T5 (mm)	T7 (mm)	T8 (mm)
8	7.2	8	7.2	8	5.2

Table 5 Key parameters of rod 3.

P (10^{-9} g/mm^3)	E_x (Gpa)	E_y (Gpa)	G_{xy} (Gpa)	$\alpha_x/10^{-6}$ °C	$a_y/10^{-6}$ °C
1.8	170.4	9.06	17.4	−1.68	16.93

Table 3 Unidirectional layer material parameters of M40 cyanate composite.

P (10^{-9} g/mm^3)	E_x (Gpa)	E_y (Gpa)	G_{xz} (Gpa)	G_{yz} (Gpa)	G_{xy} (Gpa)	$\alpha_x/10^{-6}$ °C	$a_y/10^{-6}$ °C	μ
1.8	220	9	4.5	4.5	4.5	−0.58	18.4	0.28

Table 6 Properties of truss rods made of CFRP.

	Layer angle (θ_o)	Single layer thickness (mm)	Number of layers	E_x (Gpa)	E_y (Gpa)	G_{xy} (Gpa)	A_x (10^{-6} °C)	A_y (10^{-6} °C)	Error between α_x and design value (%)
Rod 1	±17	0.2	20	154.6	9.09	20.7	−1.98	16.5	1.2
Rod 2	±15	0.2	18	170.4	9.06	17.4	−1.68	16.93	0
Rod 3	±15	0.2	20	170.4	9.06	17.4	−1.68	16.93	0
Rod 5	±15	±15	0.2	18	170.4	9.06	17.4	−1.68	16.93
Rod 6	±18	±18	0.1	30	146.2	9.12	22.4	−2.12	16.2
Rod 7	±18	±18	0.2	20	146.2	9.12	22.4	−2.12	16.2
Rod 8	±15	±15	0.2	13	170.4	9.06	17.4	−1.68	16.93

Table 7 Optical eccentricity and inclination of mirrors at 25°C condition.

	Primary mirror	Tertiary mirror	Secondary mirror	Plane mirror
ΔX (μm)	−0.011	−0.0723	0.0001	0.12
ΔY (μm)	−16.4	6.24	−33.4	−20.7
ΔZ (μm)	−5.8	−12.7	5.07	5.6
θX (″)	0.66	2.33	2.48	4.6
θY (″)	−0.035	−0.02	−0.04	−0.04
θZ (″)	−0.47	−2	−0.5	−0.7

Table 8 Eccentricity and inclination compared to primary mirror.

	Primary mirror	Third mirror	Second mirror	Plane mirror
ΔX (μm)	Datum	0.0613	0.0111	0.131
ΔY (μm)	Datum	0.023	0.017	0.0043
ΔZ (μm)	Datum	0.007	0.011	0.011
θX (″)	Datum	1.67	1.83	4
θY (″)	Datum	0.015	0.05	0.05
θZ (″)	Datum	1.53	0.03	0.23

4 FEM Analysis, Experiment, and Test Verification of the Whole Instrument

4.1 *Finite Element Analysis of the Space Telescope*

To verify whether the parameters of carbon fiber composite material designed in this paper can meet the thermal stability and dynamic properties of the telescope at 20°C ± 5°C, the parameters of Table 6 are taken into the FEM for the whole instrument analysis. Then the surface accuracy, optical eccentricity, and inclination of the mirror at 25°C are obtained and are shown in Table 7. The modal information of the whole instrument is shown in Table 8. Figure 11 shows the free expansion deformation cloud chart of the whole instrument under 25°C condition with no gravity influence.

It can be seen from Tables 7 and 8 that the optical eccentricity of each mirror compared to the primary mirror is within 0.03 mm and the inclination is within 5″, which satisfies the optical tolerance requirement in Table 1. In addition, it can be seen from Tables 7 and 8 that the optical eccentricity of the secondary mirror and the plane mirror along the optical axis (Z direction) is under control, which indicates that the front frame rotates very little around the X axis after thermal deformation. And it proves that the axial distance after thermal deformation of all truss rods is basically equal. The correctness of the design is illustrated in this paper. Finally, it can be seen that the fundamental

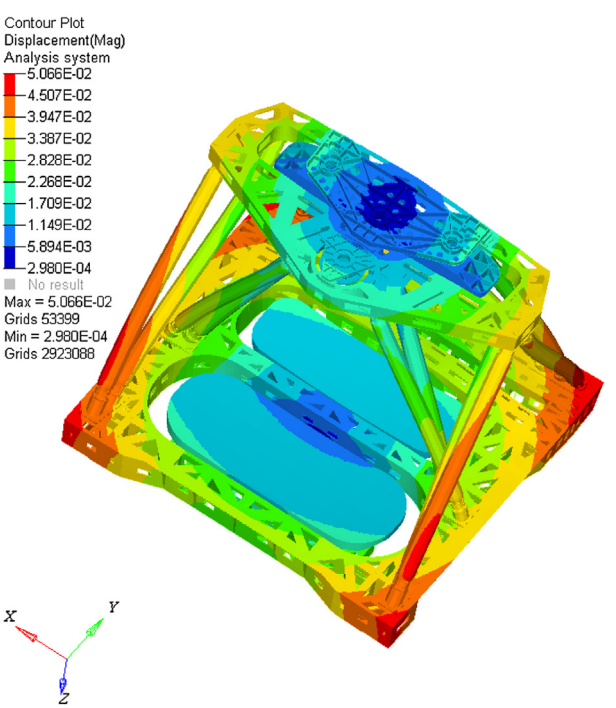

Fig. 11 Deformation cloud chart of the space telescope at 25°C.

Table 9 Modal information of the whole instrument.

Direction	Frequency (Hz)
Fundamental frequency of *X* direction	107
Fundamental frequency of *Y* direction	95.03
Fundamental frequency of *Z* direction	120

frequency of the whole instrument is up to 95 Hz, which shows that the truss structure designed in this paper has a high stiffness (Table 9).

4.2 *Vibration Experiment*

To verify the reasonableness and the correctness of the structural design of the space telescope and the finite element analysis results, the vibration experiment of the whole instrument is carried out as shown in Fig. 12, and Table 10 shows the comparison between the test results and the analysis data.

The percentage of error of finite element analysis data and vibration test data is <4%, which meets the engineering requirements. In conclusion, the FEM described in this paper is qualified and the eccentricity and tilt results of the finite element analysis are credible.

4.3 *Imaging Experiment under Thermal Conditions*

To validate the reasonableness and correctness of the thermal compensation design of the space telescope, the imaging experiment under 20°C ± 5°C thermal conditions were carried out. The test site is shown in Figs. 12 and 13. Table 11 shows the test results. In order to get a precise MTF at Nyquist frequency, the large field of view is divided into five zones laterally and equally. For every zone, at least five random points shall be measured; the average MTF of every five points of each zone shall be considered to be able to represent the MTF at Nyquist frequency (Fig. 14).

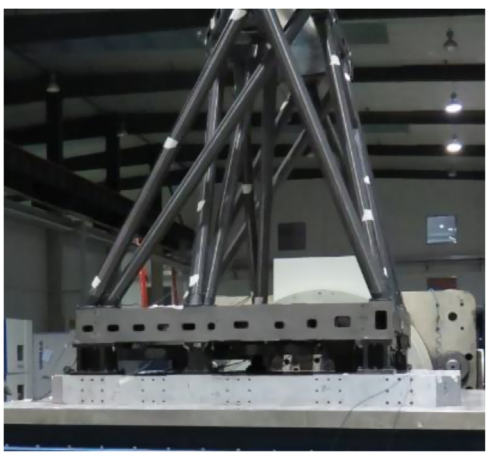

Fig. 12 Vibration experimental site.

Table 10 Comparison of vibration experiment result and analysis result.

	Analysis (Hz)	Experiment (Hz)	Error (%)
Fundament frequency of *X*	107	102.9	4
Fundament frequency of *Y*	95.03	97.2	2.2
Fundament frequency of *Z*	120	117.2	2.4

Fig. 13 Imaging experiment preparation site.

Table 11 MTF at Nyquist frequency measurement results.

	Left	Center-left	Center	Center-right	Right
MTF at 15°C	0.179	0.179	0.183	0.185	0.184
MTF at 20°C	0.193	0.195	0.220	0.196	0.192
MTF at 25°C	0.178	0.178	0.181	0.181	0.180

Fig. 14 MTF measurement of the space telescope site.

It is clearly seen from Table 11 that the MTF at Nyquist frequency of this space telescope is better than 0.175 under the temperature range of 20°C ± 5°C, which fully satisfied the MTF required by the optical system.

5 Conclusion

To satisfy the requirements of optical tolerance for the large-scale, long-focus, large field of view, TMA space telescope under thermal conditions ranging 25°C ± 5°C, a mechanical passive thermal compensation design for the supporting structure of the space telescope was carried out. Utilizing the design of composite materials, the CTE of truss rods is designed, respectively, which makes the whole instrument

structure satisfy the optical tolerance requirement after thermal deformation. At the same time, the rotation angle of the front frame around the X axis is kept at an acceptable level, which solves the problem of excessive rotation of the front panel around the X axis caused by the asymmetry of the off-axis telescope structure. Finally, the correctness and reasonableness of the design is validated by finite element analysis, vibration experiment, and imaging test. The MTF at Nyquist frequency is better than 0.178 generally.

Acknowledgments

This paper was finished with the help of my colleagues in Chang Guang Satellite company and Changchun Institute of Optics, Fine Mechanics and Physics, Chinese Academy of Sciences (CIOMP). So, I would like to thank Dr. Wei Lei, Prof. Zhang Lei who are also coauthors of this paper. Together we declare that we have no financial and personal relationships with other people or organizations that can inappropriately influence our work; there is no professional or other personal interest of any nature or kind in any product, service and/or company that could be construed as influencing the position presented in the present article.

References

1. K. Zhang, N. Ruan, and D. Fu, "Analysis and consideration of development of oversea space off-axis TMA system telescope," *Spacecraft Recovery Remote Sens.* **29**, 63–70 (2008) [in Chinese].
2. B. Fan and Y. Wang, "Research on truss structure of foreign remote-sensing telescopes with long focal length and high resolution," *Spacecraft Recovery Remote Sens.* (02), 35–41 (2008) [in Chinese].
3. B. Yang, "Characteristics and main specifications of IKONOS and QuickBird2 satellite telescope-some points for developing such like satellite telescope," *Spacecraft Recovery Remote Sens.* **23**, 14–16 (2002) [in Chinese].
4. H. Imai et al., "Conceptual design of advanced land observing satellite-3," *Proc. SPIE* **7474**, 74740R (2009).
5. Y. An and J. Yao, "Application of carbon fibre reinforced plastic for optical telescope structure," in *IEEE Int. Conf. Mechatron. and Autom.* (2012).
6. D. Li, Q. Geng, and Z. Li, "Optimization design for main supporting structure of the off-axis TMA space remote sensor," in *Int. Conf. Mech. Autom. and Control Eng.* (2010).
7. A. Bruce and T. P. O'Brien, "Adjustable truss for support, optical alignment, and athermalization of a Schmidt telescope," *Proc. SPIE* **4841**, 403–410 (2003).
8. H. Xin and Z. Li, "Structural design for lightweight off-axis TMA space telescope," in *Second Int. Conf. Digital Manuf. and Autom.* (2011).
9. T. Bret-Dibat et al., "Tests of a high-resolution three-mirror anastigmat telescope," *Proc. SPIE* **3870**, 126–137 (1999).
10. M. An, "Research on stability of the truss structure in large-scale space telescope," Changchun Institute of Optics, Fine Mechanics and Physics, Chinese Academy of Sciences (2017) [in Chinese].
11. W. Li and Q. Guo, "Application of carbon fiber composites to cosmonautic fields," *Chin. Opt.* **4**(03), 201–212 (2011) [in Chinese].
12. W. Peng, S. Sun, and G. Chen, "Lightweight design technology of space telescope optical mirror," *Opt. Tech.* **32**(Z1), 138–140 (2006) [in Chinese].
13. S. Utsunomiya, T. Kamiya, and R. Shimizu, "CFRP composite mirrors for space telescopes and their micro-dimensional stability," *Proc. SPIE* **7739**, 77392M (2010).

Lin Yang is an assistant research fellow at Changchun Institute of Optics, Fine Mechanics and Physics, Chinese Academy of Sciences, China. He received his BS degree from China University of Petroleum, his MS degree from Xi'an Jiaotong University, and his PhD from the University of Chinese Academy of Sciences. His current major research interests include spacecraft structural dynamics, optical payloads, and other optic-mechanical instruments.

Lei Wei is a PhD graduate at the University of Chinese Academy of Sciences. He received his BS degree in machine manufacturing and mechanics from Northeastern University of China in 2012. His current research interest is optomechanical structural design of space cameras.

Lei Zhang is an associate professor at CIOMP. He received his PhD in machine manufacturing and mechanics from CIOMP in 2008. His current research interest is structural design of optical remote sensing satellite.